IOP Conf. Series: Journal of Physics: Conf. Series **821** (2017) 012006 doi:10.1088/1742-6596/821/1/012006

Computation of tail probabilities for non-classical gasdynamic phenomena

N. Razaaly, P.M. Congedo

INRIA Bordeaux Sud-Ouest, 200 Rue de la Vieille Tour, 33405 Talence, France

E-mail: nassim.razaaly@inria.fr,pietro.congedo@inria.fr

Abstract. This paper presents a novel method for computing the tail probability of a given quantity of interest by using only a low number of evaluations of the computer model, representing the problem of interest under uncertainties. This method is then applied to the study of rarefaction shock waves (RSW) in a dense-gas shock tube. It is well-known in literature that the prediction of a RSW is highly sensitive to uncertainties on the initial flow conditions. The objective of this work is to compute a very accurate estimation of the RSW probability of occurrence in a shock tube configuration.

1. Introduction

Several theoretical and numerical studies have shown that dense-vapor transonic flows of substances formed by complex organic molecules could feature phenomena such as rarefaction shock waves and compression fans. Fluids that might exhibit nonclassical gasdynamic phenomena are called BZT fluids from the name of the three scientists who first theorized their existence. These anomalies occur when the fundamental derivative of gasdynamics $\Gamma = 1 + \frac{\rho}{a}\left(\frac{\partial a}{\partial \rho}\right)_s$ with ρ the fluid density, a the sound speed and s the entropy, becomes negative between the upper saturation curve and the $\Gamma = 0$ contour. Such a region is often referred to as the *inversion zone* and and the $\Gamma = 0$ contour is called the *transition line*.

The experimental proof of nonclassical gasdynamic effects in flows of dense vapors has been the subject of several studies [2, 3, 1], most of all focused on a shock tube configuration for generating a rarefaction shock wave (RSW). These works show that nonclassical gasdynamic effects are generally very weak with respect to compression shock waves, and can occur only in a limited range of conditions. As shown for instance in [4] and [5], the accuracy of the thermodynamic model has a strong influence on the simulation of nonclassical phenomena, to the point that their presence can depend on the accuracy with which fluid model parameters are determined.

In [1], an algorithm has been presented to handle stochastic inverse problem with high efficiency and a reduced computational cost. This algorithm has then been applied to the design of a challenging scientific experiment involving the compressible flow of a dense gas in the FAST shock tube facility at TU Delft. It was shown that the unconventional rarefaction shock wave is very sensitive to uncertainties in the initial experimental conditions.

This paper is focused to cure some of the issues emerged in [1]. The difficulties to accurately compute the tail probability and the associated computational cost are tackled with a novel

uncertainty quantification techniques, based on an interpolation technique and an importance sampling algorithm. The final algorithm is then applied to the simulation of the TU Delft experiments.

The paper is organized as follows. Section 2 is devoted to the description of the various numerical tools needed in the study: the CFD solver for dense gas flows simulations, the thermodynamic models, and the uncertainty quantification approach. In section 2.4, the stochastic method is presented. Section 3 illustrates some results obtained on the computation of the tail probability of the RSW. The closing section summarizes the conclusions that can be drawn from the present work.

2. Methodology and tools

2.1. CFD solvers for dense gas flows

The NZDG code [1] solves the quasi-1D Euler equations with second-order accuracy in time and space. The convective fluxes are discretized using the Roe numerical flux and a second-order limited MUSCL variable reconstruction. The Roe average for dense gas flows is computed with the simplified approach proposed in [6] and the slope limiter introduced in the linear reconstruction is of the Van Albada type. Second-order accuracy in time and robust time-integration are achieved using a three-level implicit formula to approximate the physical time-derivative, within a dual-time sub-iterative approach to solve the resulting non-linear system.

2.2. Thermodynamic models

Siloxane D6 is the fluid currently chosen for the TU Delft experiment. The $Peng - Robinson - Strijek - Vera$ (PRSV) cubic equation of state (EoS) is considered to describe its thermodynamic behavior. The robustness of this equation with respect to more complex and potentially more accurate multi-parameter equations of state of the Span-Wagner type ([5],[7],[4] has been discussed in [8] and [9]. Peng and Robinson (1976) proposed a cubic EoS of the form:

$$p = \frac{RT}{v-b} - \frac{a}{v^2 + 2bv - b^2}. \tag{1}$$

where p and v denote respectively the fluid pressure and its specific volume, a and b are substance-specific parameters related to the fluid critical-point properties p_c and T_c. To achieve high accuracy for saturation-pressure estimates of pure fluids, the temperature-dependent parameter a in Eq.(2.1) is expressed as :

$$a = \left(0.457235 R^2 T_c^2 / p_c^2\right) \cdot \alpha\left(T\right) \tag{2}$$

while

$$b = 0.077796 R T_c / p_c \tag{3}$$

These properties are not completely independent, since the EoS should satisfy the conditions of zero curvature and zero slope at the critical point. Such conditions allow computing the critical compressibility factor $Z_c = (p_c v_c)/(RT_c)$ as the solution of a cubic equation. The corrective factor α is given by:

$$\alpha\left(T_r\right) = \left[1 + K\left(1 - T_r^{0.5}\right)\right]^2 \tag{4}$$

with

$$K = K_0 + K_1\left(1 + T_r^{0.5}\right)\left(0.7 - T_r\right) \; for\, T_r < 1 \;\; \left(K_1 = 0, for\, T_r \geq 1\right) \tag{5}$$

and

$$K_0 = 0.378893 + 1.4897153\omega - 0.1713848\omega^2 + 0.0196554\omega^3. \tag{6}$$

The parameter ω is the fluid acentric factor and K_1 is obtained from saturation-pressure fitting of experimental data. The caloric behavior of the fluid is approximated through a power law for the isochoric specific heat in the ideal gas limit:

$$c_{v,\infty}(T) = c_{v,\infty}(T_c)\left(\frac{T}{T_c}\right)^n \tag{7}$$

with n a material-dependent parameter.

2.3. Sources of Uncertainty : initial conditions of the experiment
The initial conditions (IC) for the experiment (and for the simulation) are prescribed according to the theory described in [10], to maximize the Mach number of the rarefaction shock wave and facilitate the wave detection. The maximum achievable precision in controlling the temperature and pressure values in the charge tube has been estimated from the measurement instruments and hardware specifications to be 0.4% for the pressure and 0.1% for the temperature.

In [1], an automatic procedure has been set up to detect an initial left state satisfying the aforementioned requirements : in the first step, a discretization of the p-v plane has been generated by moving along isobaric and isentropic curves; in the second step, the uncertainty region is computed using the given uncertainty levels on initial pressure and temperature and a Monte-Carlo approach; in the third step, it is verified the uncertainty region does not cross the saturation curve (to avoid liquid-vapor mixture) and that the chosen point is located as close as possible to the saturation curve. This analysis yields an initial left state, denoted P1, represented in figure 1. The uncertainty region for P1 has a single point in common, without crossing, with the maximal allowed saturation curve computed with the TD uncertainties taken into account.

2.4. Stochastic method
In the following, we describe a new stochastic method specifically designed to accurately compute very low probability subject to multiple failure regions. The idea is to construct a metamodel of the quantity of interest specially refined on the failure branches, and then resort to a sampling-based method on the metamodel in order estimate the probability of failure.

2.4.1. Introduction Given a probabilistic model, described by its physical n-dimensional random vector $\mathbf{Y}$ with its probability density function (PDF) $f_{\mathbf{Y}}$ and a performance function J representing the system response, failure is usually defined as the event $\mathcal{G} = \{J(\mathbf{y}) \leq 0\}$ so that the failure probability is defined as follows:

$$p_f = \mathbb{P}([J(\mathbf{Y}) \leq 0]) = \mathbb{E}_{\mathbf{Y}}[\mathbb{1}_{\mathcal{G}}(\mathbf{Y})] = \int_{\mathbb{R}^n} \mathbb{1}_{\mathcal{G}}(\mathbf{y}) f_{\mathbf{Y}}(\mathbf{y}) d\mathbf{y} \tag{8}$$

where $\mathbb{1}_{\mathcal{G}}$ is the failure indicator function, being equal to one if $J(\mathbf{y}) \leq 0$, and zero otherwise. J is called the performance function in this paper. An isoprobabilistic transformation T (e.g. Rosenblatt transform) is used to define the standard random variables X and the performance function G in the standard space as $G(X) = J(T^{-1}(X))$ with $X = T(Y)$.

We recall that $X \sim \mathcal{N}(0, I_n)$ is the standard normal random vector of $\mathbb{R}^n$. The failure domain $\mathcal{F}$ in the standard space is then defined as $\mathcal{F} = \{\mathbf{x} \in \mathbb{R}^n \ \ s.t. \ \ G(x) < 0\}$. The failure probability reads

$$p_f = \mathbb{P}([G(\mathbf{X}) \leq 0]) = \mathbb{E}[\mathbb{1}_{\mathcal{F}}(\mathbf{X})] = \int_{\mathbb{R}^n} \mathbb{1}_{\mathcal{F}}(\mathbf{x}) f_{\mathbf{X}}(\mathbf{x}) d\mathbf{x} \tag{9}$$

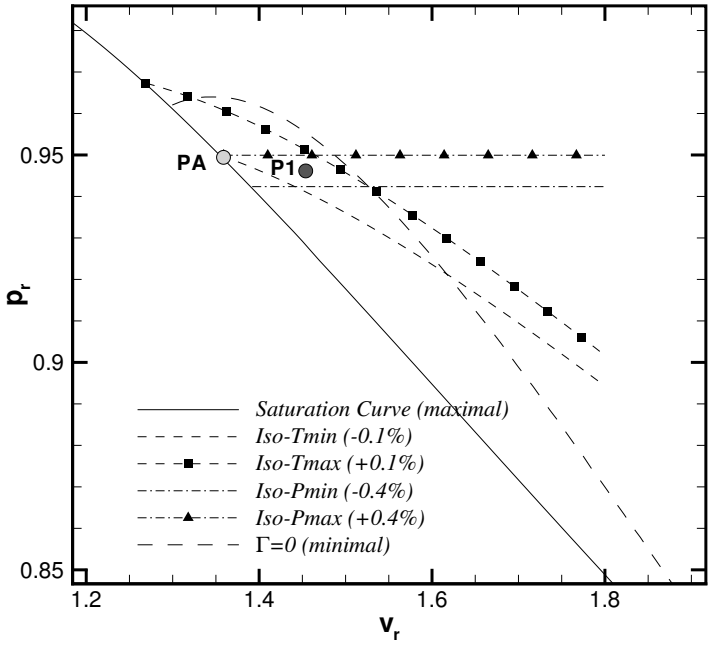

Figure 1: Robust point (P1) obtained by means of the automatic procedure, and uncertainty region.

Computing failure analysis in the standard space simplifies the analysis since, the random variables are decorrelated and normalized.

A typical approach to the estimation of the failure probability (Eq. 9) is that of resorting to a crude Monte Carlo (MC) scheme. It yields to an unbiased and convergent estimation of p_f, with a low convergence rate. It usuaally requires a prohibitive number of simulations.
Various methods have been proposed in the literature to adress this problem.
A first family of method aims to reduce the variance estimator in order to increase the convergence rate. Importance sampling techniques [11] [12] are part of this family, and have been developed over the past few decades to shift the underlying distribution towards the failure region so as to gain information from rare events more efficiently. The success of the method relies on a prudent choice of the importance sampling density, which undoubtedly requires knowledge of the system in the failure region.
The second class of methods relies on the substitution of the original performance function by a surrogate model within a sampling-based scheme; a metamodel is in general orders of magnitude faster to be evaluated. In such metamodel-based approaches, Monte-Carlo sampling (AK-MCS [17]) or Importance Sampling (IS) techniques (AK-IS [13], MetaAK-IS^2 [14], KAIS [15], AK-SS [16]) are then used directly on the surrogate. Here, we propose a new method for the metamodel construction. It makes the use of the learning function used in AK-MCS [17], k-Means clustering algorithm [18], and a Metropolis-Hastings MCMC sampling method [19]. It is designed to fit with multiple failure regions, and very low probability. It provides few advantages compared to other metamodels refinement:

- A parameter is used to avoid points clustering and also give the opportunity for the user to indirectly control the refinement cost.

- The different failure-branches are refined back and forth during the process. So if the number of DOE required during the metamodel building is too high (impossibility to build a metamodel for instance), the resulting metamodel will be "equally" refined in all branches.
- It focuses on the limit state performance function.

This section is organized as follows. The concept of probabilistic classification and of importance sampling are presented in Sections 2.4.2 and 2.4.3, respectively. The metamodel refinement strategy is detailed in subsection 2.4.4. An academic test-case for validation is discussed in subsection 2.4.5.

2.4.2. Probabilistic classification using Gaussian Processes A metamodel is built from a *design of experiments* (D.o.E.), a set of computed experiments denoted by $\mathcal{X} = \{\mathbf{x}_1, ..., \mathbf{x}_m\}$, belonging to the support $\mathcal{D}_{\mathbf{x}}$ of $\mathbf{X}$. The performance function G is assumed to be a sample path of an underlying Gaussian Process (GP) denoted by $\tilde{G}$. The *best linear unbiased estimation* (BLUE, see [20]) of $\tilde{G}$ at point $\mathbf{x}$ is shown to be a Gaussian random variate $\hat{G}(\mathbf{x}) \sim \mathcal{N}(\mu_{\hat{G}(\mathbf{x})}, \sigma_{\hat{G}(\mathbf{x})})$, where $\mu_{\hat{G}(\mathbf{x})}, \sigma_{\hat{G}(\mathbf{x})}$ are given by the Gaussian Process algorithm. Further details can be found in [21].
GP provides both a surrogate for the limit-state function $g(\mathbf{x})$ which is denoted by $\mu_{\hat{G}(\mathbf{x})}$ and an epistemic prediction uncertainty which is characterized by its variance $\sigma^2_{\hat{G}(\mathbf{x})}$.

We introduce the *probabilistic classification function*:

$$\pi(\mathbf{x}) = \mathcal{P}[\hat{G}(\mathbf{x}) \leq 0] = \phi\left(\frac{0 - \mu_{\hat{G}(\mathbf{x})}}{\sigma_{\hat{G}(\mathbf{x})}}\right), \text{ if } \mathbf{x} \notin \mathcal{X} \tag{10}$$

where the probability measure $\mathcal{P}[\cdot]$ refers to the Gaussian nature of the GP predictor $\hat{G}(\mathbf{x})$ and ϕ denotes the *cumulative density function* of the one-dimensional standard normal law. It may be interpreted as the probability that the predictor $\hat{G}(\mathbf{x})$ is negative with respect to the epistemic uncertainty. We will later use π as a surrogate for $\mathbb{1}_{\mathcal{F}}$.
We also introduce the meta-failure domain $\tilde{\mathcal{F}}$ in the standard space, defined as $\tilde{\mathcal{F}} = \left\{\mathbf{x} \in \mathbb{R}^n \;\; s.t. \;\; \mu_{\hat{G}(x)} < 0\right\}$.

2.4.3. Importance Sampling and Quasi-Optimal Density Let h be a PDF dominating $\mathbb{1}_{g\leq 0} f_{\mathbf{X}}$. The failure probability may be rewritten as follows:

$$p_f = \int_{\mathbb{R}^n} \mathbb{1}_{g\leq 0}(\mathbf{x}) \frac{f_{\mathbf{X}}(\mathbf{x})}{h(\mathbf{x})} h(\mathbf{x}) d\mathbf{x} = \mathbb{E}_h[\mathbb{1}_{g\leq 0}(\mathbf{X}) \frac{f_{\mathbf{X}}(\mathbf{X})}{h(\mathbf{X})}] \tag{11}$$

It easily leads to the *importance sampling estimator*:

$$\hat{p}_{f\ IS} = \frac{1}{N} \sum_{k=1}^{N} \mathbb{1}_{g\leq 0}(\mathbf{x}^{(k)}) \frac{f_{\mathbf{X}}(\mathbf{x}^{(k)})}{h(\mathbf{x}^{(k)})} \tag{12}$$

where $\{\mathbf{x}^{(1)}, ..., \mathbf{x}^{(N)}\}$ is a set of samples drawn from the instrumental density h. According to the central limit theorem, this estimation is unbiased and its quality may be measured by means of its variance of estimation which reads

$$Var[\hat{p}_{f\ IS}] = \frac{1}{N-1}\left(\frac{1}{N} \sum_{k=1}^{N} \mathbb{1}_{g\leq 0}(\mathbf{x}^{(k)}) \frac{f_{\mathbf{X}}(\mathbf{x}^{(k)})^2}{h(\mathbf{x}^{(k)})^2} - \hat{p}^2_{f\ IS}\right) \tag{13}$$

The corresponding coefficient of variation is defined as $\hat{\delta}_{p_f} = \frac{\sqrt{Var[\hat{p}_{f\ IS}]}}{\hat{p}_{f\ IS}}$.

This variance is zero (optimality of the IS estimator) when the instrumental PDF is chosen as $h^*(\mathbf{x}) = \frac{\mathbb{1}_{g\leq 0}(\mathbf{x}) f_{\mathbf{X}}(\mathbf{x})}{p_f}$.

However, this PDF involves p_f in its denominator, so it is not implementable in practice. Here, it is proposed to use the probabilistic classification function (Eq. 10) as a surrogate for the real indicator function $\mathbb{1}_{g\leq 0}(\mathbf{x})$. The proposed quasi-optimal PDF reads $\hat{h^*}(\mathbf{x}) = \frac{\pi(\mathbf{x}) f_{\mathbf{X}}(\mathbf{x})}{\mathbb{E}_{\mathbf{X}}[\pi(\mathbf{X})]}$, where $\mathbb{E}_{\mathbf{X}}[\pi(\mathbf{X})]$ can be evaluated with crude Monte-Carlo method.
Markov chain Monte Carlo (*Metropolis-Hastings sampler*) simulation [19] is used in the next subsubsection to sample points drawn from from the quasi-optimal instrumental PDF $\hat{h^*}$, that are more likely to be close to limit-state.

2.4.4. Metamodel Refinement Strategy The efficiency of the approach mostly relies on the optimality of the instrumental PDF $\hat{h^*}$. Thus it is proposed here to adaptively refine the probabilistic classification function so that the quasi-optimal instrumental PDF $\hat{h^*}$ converges towards its optimal counterpart h^*.

A learning function U [14] associated to the GP metamodel $\hat{G}$ is introduced. For a given $\mathbf{x}$, $U(\mathbf{x})$ is defined as

$$U(\mathbf{x}) = \frac{|\mu_{\hat{G}(\mathbf{x})}|}{\sigma_{\hat{G}(\mathbf{x})}} \tag{14}$$

$\phi(U(\mathbf{x}))$ is the probability that $\mathbf{x}$ is correctly classified by the predictor. So if N points $\mathbf{x}(i)$ are available,

$$\mathbf{x}_0 = \arg\min_i (U(\mathbf{x}(i))) \tag{15}$$

is the point in correspondence of which the classification is the most uncertain. In order to avoid DOE clustering, a constraint is added, stating that $\mathbf{x}_0$ should be distant of at least d_{min} from all existing DOE. The algorithm proceeds as follows:

(i) *Initial DOE and metamodel definition*: sample m_0 points generated by a Latin Hypercube sampling.

(ii) *Sampling*: Sample a Monte-Carlo population $\mathcal{N} = \{x^{(1)}, ..., x^{(N)}\}$, adapting N so a coefficient target of variation is reached.

(iii) *Global Point Selection*: Refine and update the metamodel selecting the best point among $\mathcal{N}$ according to the learning function U.

(iv) *Classification*: Classify $\mathcal{N}$ between failure and safe points.

(v) *Seed Selection*: Use k-Means [18] clustering algorithm on the set of failure points. Its K clusters centroids are considered: $(x_1^-, ..., x_K^-)$. Set $k = 1$.

(vi) *Unimodal MCMC Sampling*: Sample a set of N_{MCMC} points $\mathcal{S}_k^{MCMC}$ drawn from the PDF $h^*_{\tilde{G}}$ using the modified MCMC Metropolis-Hastings sampler, with the seed initialized at x_k^-. Burning and thining procedure are used. Remove the first N_{MCMC}^{min} values obtained, and then, accept only one sample every s_{MCMC} samples.

(vii) *Enrich D.o.E. at step k*: Select the best point $\{\tilde{x}_k^-\}$ (if exists) among $\mathcal{S}_k^{MCMC}$ according to the learning function U. Update the metamodel.

(viii) *Stopping criterion* If $k \neq K$: set $k = k + 1$ and loop back to step vi.
If $k = K$ and $\bigcup_{k=1}^{K} \{\tilde{x}_k^-\} = \varnothing$, stop the metamodel refinement algorithm.
Otherwise, set $i = i + 1$ and loop back to step ii.

The metamodel refining procedure stops when no more points can be added. In order to evaluate the probability of failure once the metamodel is refined, it is possible to resort to Monte-Carlo method if p_f is low enough. Otherwise, it is proposed to use the Importance Sampling method, with a gaussian mixture density as the Importance Sampling Density. MCMC points are sampled from different seeds in parallel, and then classified using k-Means algorithm. The gaussian mixture parameters: weights, means, covariance are then empirically computed from those classified MCMC points.

2.4.5. Validation: 2D analytic example with four failure regions We test the method in case of four failure regions. The performance function [14] [22] in the standard space reads:

$$G(x_1, x_2) = \min \left\{ \begin{array}{c} 3 + \frac{(x_1 - x_2)^2}{10} - \frac{x_1 + x_2}{\sqrt{2}} \\ 3 + \frac{(x_1 - x_2)^2}{10} + \frac{x_1 + x_2}{\sqrt{2}} \\ x_1 - x_2 + \frac{7}{\sqrt{2}} \\ -(x_1 - x_2) + \frac{7}{\sqrt{2}} \end{array} \right\} \tag{16}$$

where x_1, x_2 are the realizations of two independent standard Gaussian random variables.

The results in Table 1, are compared to those reported in [14] [17]: crude MC, FORM, DS, Subset, SMART, MetaAK-IS^2 and AK-MCS+U. The method proposed shows a good accuracy, with less performance calls than the other methods.

Method	N_{calls}	$\hat{p}_f$	$\hat{\delta}_f$
Crude MC	$781,016$	2.24×10^{-3}	2.23%
FORM	7	1.35×10^{-3}	
DS	1800	2.22×10^{-3}	
Subset	$600,000$	2.22×10^{-3}	1.5%
SMART	1035	2.21×10^{-3}	
MetaAK-IS^2	138	2.22×10^{-3}	1.7%
AK-MCS+U	96	2.23×10^{-3}	
MetaAL-OIS	$\mathbf{15 + 61}$	$\mathbf{2.23 \times 10^{-3}}$	**0.09%**

Table 1: Comparison of the performances of the MetaAL-OIS with several algorithms of literature[14].

Figure 2 compares the limit-state obtained by the metamodel, to the true limit-state.

3. Application to the shock tube

The meta-model refinement of the meta-IS algorithm is applied to the estimation of the failure probability of the experiment, *i.e.* the probability of the pre-shock Mach number, in the reference frame attached to the shock, to be less than one. Indeed, this Mach associated to the rarefaction shock wave is required to be larger than one for the shock to be well measured. In this configuration, the performance function can be then defined as follows

$$G(p_L, p_R) = M - 1, \tag{17}$$

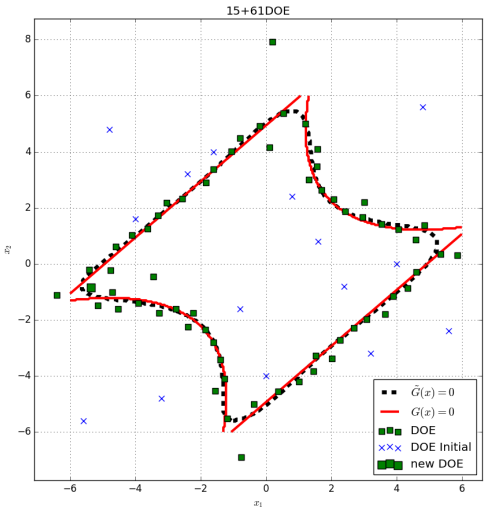

Figure 2: 2D analytic example with four failure regions: Refined Metamodel with 76 points.

p_L, p_R being respectively the left and right pressure. M denotes the Mach number associated to the RSW. The failure event is

$$p_f = \mathbb{P}(G(p_L, p_R) < 0) = \mathbb{P}(M(p_L, p_R) < 1) \tag{18}$$

where p_L, p_R are assumed to be two independent adimensioned random variables (Table 2), according to the uncertainty assessment.

Variable	**Distribution**	**Minimum**	**Maximum**
p_L	Uniform	0.908	0.984
p_R	Uniform	0.099	0.108

Table 2: Probabilistic model for the shock tube

The application of the algorithm presented in the previous section permits to compute the metamodel of the Mach number associated to the RSW, indicated as $\hat{M}$ in the following. By sampling the metamodel, several analysis are possible in terms of statistics evaluation. Results about the tail probability computations and some statistics associated to the Mach number are summarized in table 3.

Note that the failure probability, *i.e.* $M < 1$, is of 43.5%, where the variance of the estimator amounts to the 0.16%. This means that the tail probability is very well computed, and indicates a very large failure probability in terms of occurrence of a RSW during the experiment.

A plot of the probability density function (PDF) of the Mach number is shown 3, where some of the properties in terms of expected value, variance and 90% confidence interval, are reported in Table 3. Also, plots of the metamodel refined in the standard and its contour in the physical spaces are shown in Figures 4a and 4b. Note that the PDF features a not-gaussian behavior, it is very skewed towards the lower Mach, confirming the large probability that the experiment is not effective because of the low value of the Mach. This is a confirmation of the results obtained in [1], even if the shape of the PDF and the associated failure probability is slightly different. This could be associated to the limited number of samples used in [1] for

computing the Polynomial-chaos based metamodel, which could deteriorate the computation of the low-probability events. Note that the presented tool provides a very fast estimation of the failure of the experiment, permitting potentially the investigation of a large set of conditions at a very low computational cost.

N_{calls}	$\hat{p}_f$	$\delta_{\hat{p}_f}$
$20 + 7$	0.435	0.16 %
$\mu_{\hat{M}}$	$\sigma^2_{\hat{M}}$	90% confidence interval
1.0072006	5.271×10^{-4}	0.9745-1.0466

Table 3: Tail probability estimation and Mach number statistics

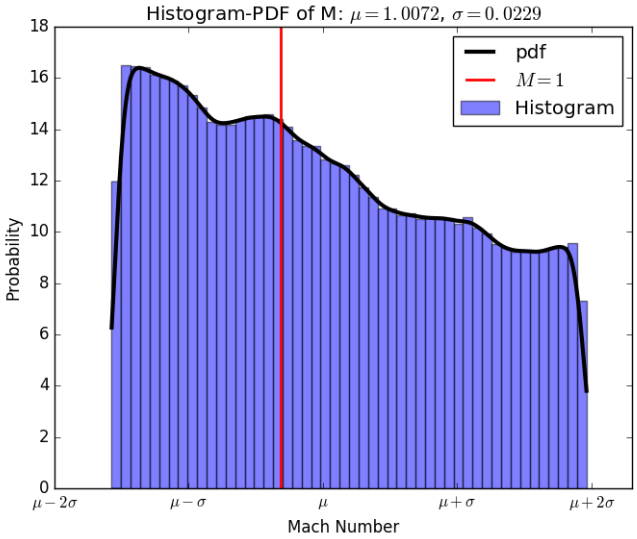

Figure 3: PDF of the Mach Number associated to the Rarefaction Shock Wave.

4. Conclusions

This paper illustrates a novel method for computing the tail probability of a given quantity of interest by using only a low number of evaluations of the computer model. This algorithm is applied to the prediction of the occurrence of a rarefaction shock wave (RSW) in a shock tube configuration, since the computation of the tail probability of the Mach associated to the RSW is very sensitive to the initial conditions uncertainty.

Results show that the occurrence of the RSW is around the 56%, which is quite low and makes questionable the repeatability of the experiment for the chosen initial conditions. This highlights the importance of assessing uncertainty when weak effects, as those associated to a non-classical gasdynamics, have to be captured. Otherwise, the risk is to overestimate the quality of the numerical experiments, which could be very sensitive to some conditions, and provide in practice low-probability results. The low number of evaluations, which are needed to compute the tail probability, illustrates the potentialities of the proposed stochastic method. Also, it should be mentioned that there is no limitation to apply this stochastic method, taking account for uncertainties with the parameters of the thermodynamic model adopted to describe the fluid.

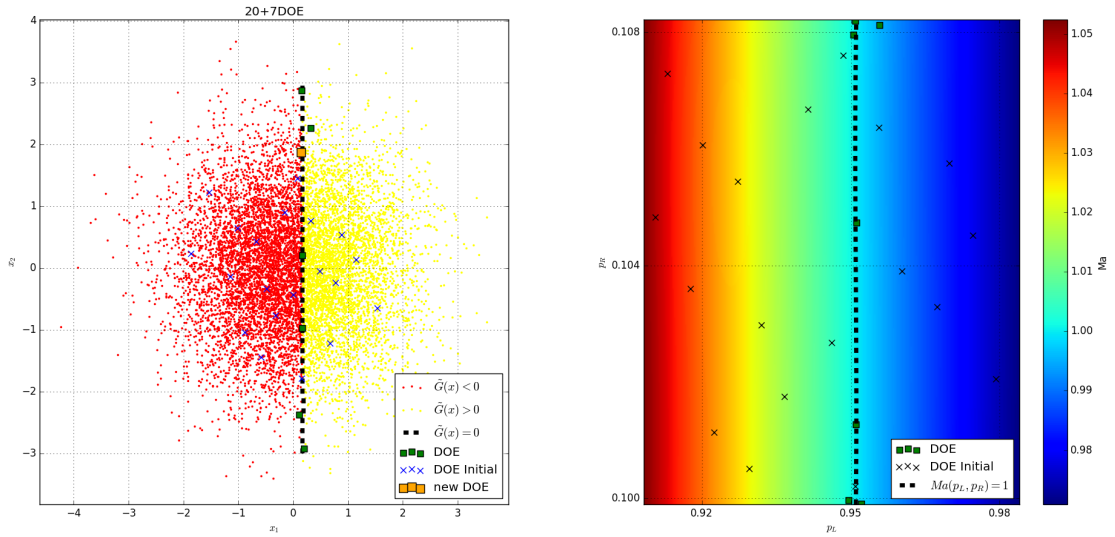

(a) Monte-Carlo population classified by the metamodel $\tilde{G}$ in the standard Space

(b) Metamodel Contour in the physical space: Mach number as function of p_L and p_R

Figure 4: Shock Tube: Refined Metamodel.

Future works will be oriented to the optimization of the geometry and the initial conditions in order to maximize the probability of occurrence of the RSW.

References

[1] Congedo PM, Colonna P, Corre C, Witteveen J and Iaccarino G 2012 *Computer Methods in Applied Mechanics and Engineering* **213** 314-326
[2] Colonna P, Guardone A, Nannan NR and Zamfirescu C 2008 *J. Fluid Eng.-T. ASME.* **130** 1-6
[3] Colonna P, Guardone A, Nannan NR and Van der Stelt TP 2009 *Fluid Phase Equilib.* **286** 43-54
[4] Colonna P, Nannan NR and Guardone A 2008 *Fluid Phase Equilib.* **263** 115-130
[5] Colonna P, Nannan NR, Guardone A and Lemmon EW 2006 *Fluid Phase Equilib.* **244** 193-211
[6] Cinnella P 2006 *Computers and Fluids* **35** 1264-1281
[7] Colonna P, Guardone A and Nannan NR 2007 *Phys. Fluids* **19086102** 1-12
[8] Cinnella P, Congedo PM, Pediroda V and Parussini L 2010 *International Journal of Engineering Systems Modelling and Simulation* **2** 12-24
[9] Congedo PM, Corre C and Martinez JM 2011 *Comput. Methods Appl. Mech. Engrg.* **200** 216-232
[10] Guardone A, Zamfirescu C and Colonna P 2010 *J. Fluid Mech.* **642** 127-146
[11] Rubinstein RY 1981 *Simulation and the Monte-Carlo method* (New York: Wiley)
[12] Fishman GS 1996 *Monte-Carlo: concepts, algorithms, and applications* (New York: Wiley)
[13] Echard B, Gayton N, Lemaire M and Relun N 2013 *Reliability Engineering and System Safety* **111** 232-240
[14] Cadini F, Santos F and Zio E 2014 *Reliability Engineering and System Safety* **131** 109-117
[15] Zhao H, Yue Z, Liu Y, Gao Z and Zhang Y 2015 *Applied Mathematical Modelling* **39** 1853-66
[16] Huang X, Chen J and Zhu H 2016 *Structural Safety,* **59** 86-95
[17] Echard B, Gayton N and Lemare M 2011 *Reliability Engineering and System Safety,* **33** 145-154
[18] MacQueen J 1967 *Proceedings of the Berkeley symposium on mathematical statistics and probability* **1** 281-97
[19] Au SK and Beck J 2001 *Prob. Eng. Mech.,* **16** 263-77
[20] Santner T, Williams B and Notz W 2003 *The design and analysis of computer experiments* (New York: Springer)
[21] Rasmussen CE and Williams C 2006 *Gaussian Processes for Machine Learning* (MIT Press)
[22] Dubourg V, Sudret B and Deheeger F 2013 *Probabilistic Engineering Mechanics,* **33** 47-57